

Supporting Information to the manuscript:

**Key aromatic/hydrophobic amino acids controlling a cross-amyloid peptide interaction versus amyloid self-assembly**

Maria Bakou, Kathleen Hille, Michael Kracklauer, Anna Spanopoulou, Christina V. Frost, Eleni Malideli, Li-Mei Yan, Andrea Caporale, Martin Zacharias and Aphrodite Kapurniotu

## Table of contents

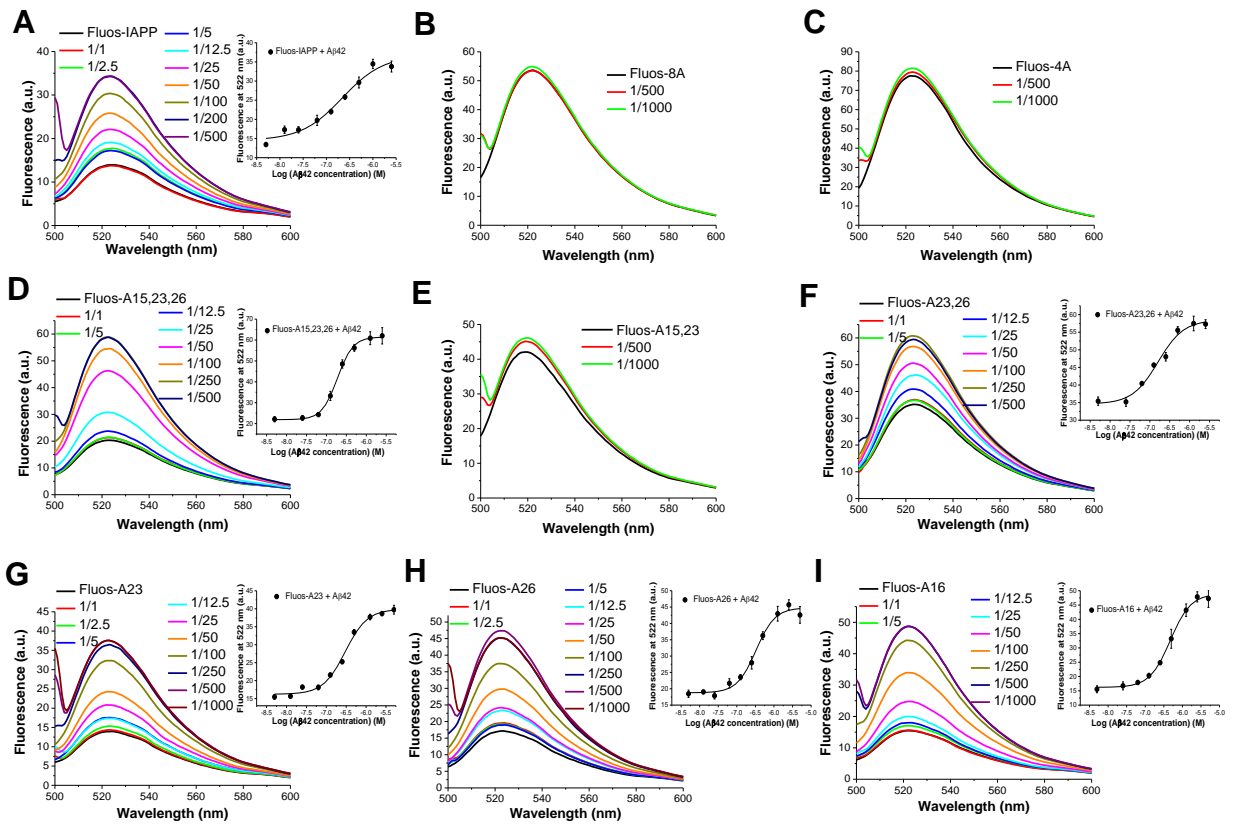
<b>Title and authors</b>	S-1
<b>Table of contents</b>	S-2
<b>Supporting Tables</b>	
<b>Supporting Table 1:</b> Average RMSD and SASA values from MD simulation.	S-3
<b>Supporting Figures</b>	S-4 – S-9
<b>Supporting Figure S1.</b> Determination of app. $K_{d,s}$ of interactions of IAPP and selected mutants with A $\beta$ 42 via fluorescence spectroscopic titrations.	S-4
<b>Supporting Figure S2.</b> Determination of app. $K_{d,s}$ of interactions of IAPP and selected mutants with IAPP via fluorescence spectroscopic titrations.	S-5
<b>Supporting Figure S3.</b> Pull-down assays of Biotin-4A-A $\beta$ 42 and Biotin-IAPP-A $\beta$ 42 hetero-assemblies.	S-6
<b>Supporting Figure S4.</b> Effects of IAPP-GI and its Ala mutants on amyloidogenesis of A $\beta$ 40, A $\beta$ 42 and IAPP.	S-7
<b>Supporting Figure S5.</b> Solubilities of A15,23 and single Ala mutants at 50 and 20 $\mu$ M, respectively (aq. buffer, pH 7.4).	S-8
<b>Supporting Figure S6.</b> Calculated secondary structure contents of IAPP and its mutants at peptide concentrations 5-50 $\mu$ M via deconvolutions of CD spectra.	S-9

## Supporting Tables

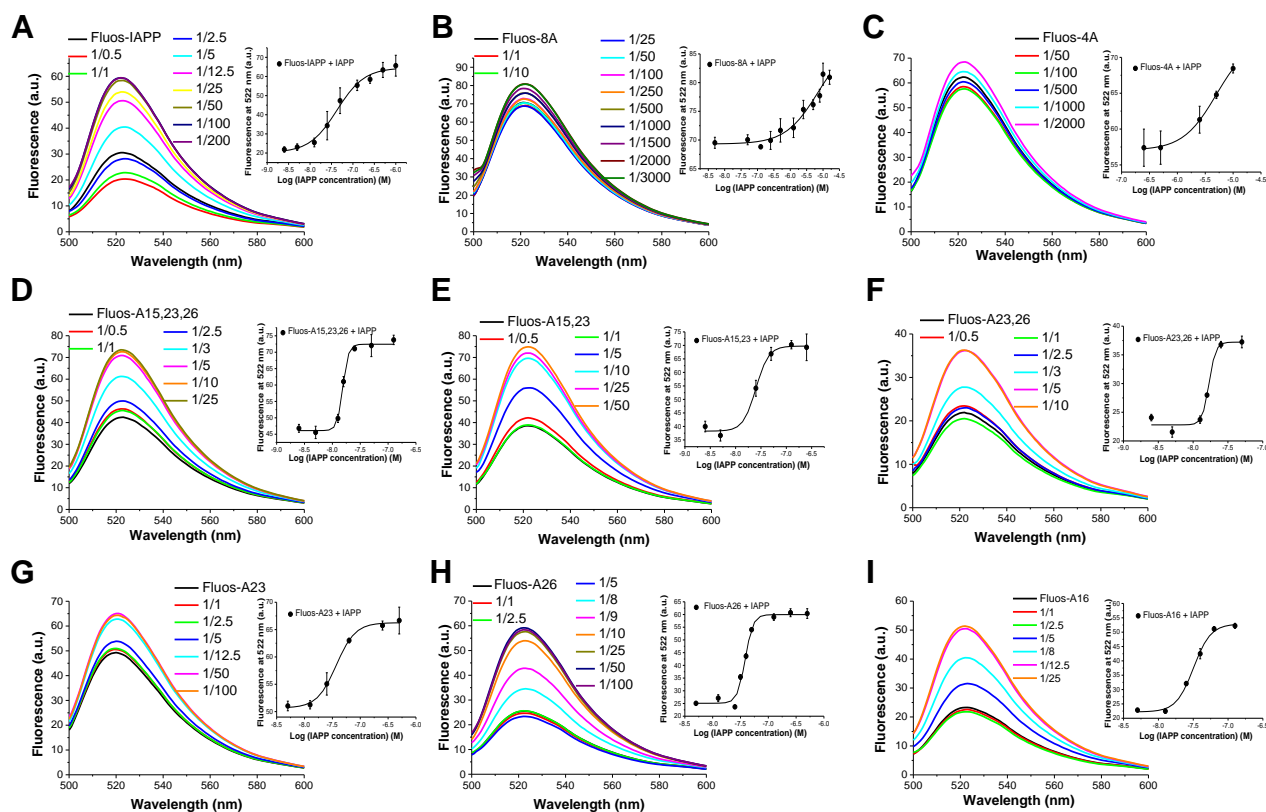
**Supporting Table 1.** Mean value ( $\pm$ SD) of C $\alpha$ -atom root-mean-square deviation (RMSD) and solvent-accessible surface area (SASA) calculated from MD simulation (3  $\mu$ s).

<b>IAPP &amp; mutants</b>	<b>C<math>\alpha</math>-RMSD (<math>\text{\AA}</math>)</b>	<b>SASA (<math>\text{\AA}^2</math>)</b>
IAPP	1.31 ( $\pm$ 0.1)	205 ( $\pm$ 57)
A23	1.13 ( $\pm$ 0.1)	318 ( $\pm$ 103)
A26	1.44 ( $\pm$ 0.2)	159 ( $\pm$ 73)
A15,23	1.15 ( $\pm$ 0.1)	282 ( $\pm$ 87)
4A	2.68 ( $\pm$ 0.2)	568 ( $\pm$ 145)

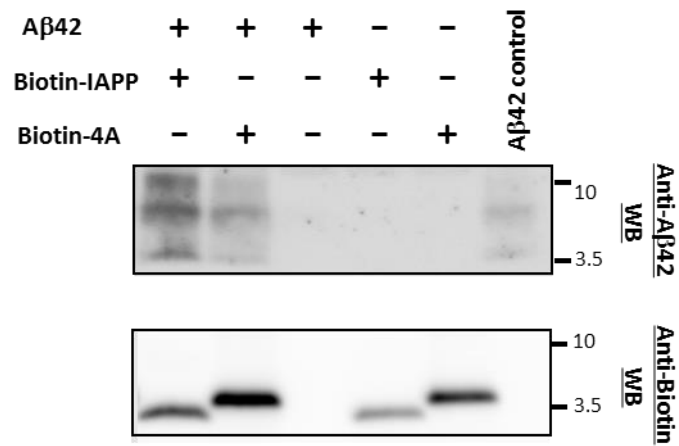
## Supporting Figures



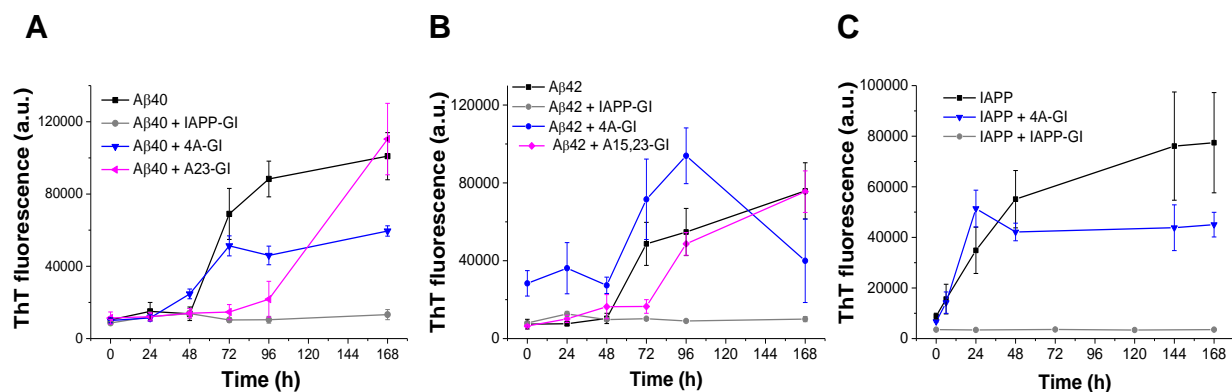
**Supporting Figure S1.** Determination of app.  $K_{d}$ s of interactions of IAPP and selected Ala mutants (5 nM) with Aβ42 by fluorescence spectroscopic titrations. Fluorescence emission spectra of N<sup>α</sup>-terminal fluorescein-labeled IAPP or mutants (Fluos-peptide) alone and after titration with Aβ42 (Fluos-peptide/Aβ42 as indicated) are shown for the following peptides: (A) IAPP; (B) 8A; (C) 4A; (D) A15,23,26; (E) A15,23; (F) A23,26; (G) A23; (H) A26; (I) A16. In the insets, the binding curves are shown; data are means ( $\pm$ SD) from three binding curves. Calculated app.  $K_{d}$ s are in Table 2.



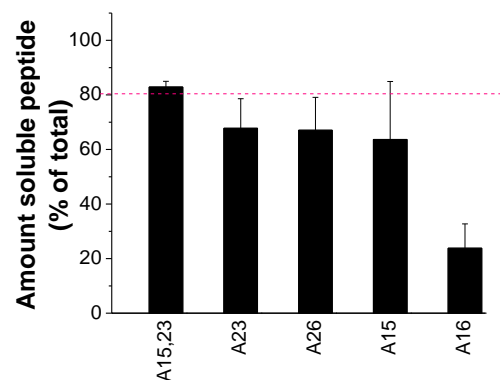
**Supporting Figure S2.** Determination of app.  $K_{d}$ s of interactions of IAPP and selected Ala mutants (5 nM) with IAPP by fluorescence spectroscopic titrations. Fluorescence emission spectra of N<sup>α</sup>-terminal fluorescein-labeled IAPP or mutants (Fluos-peptide) alone and after titration with IAPP ((molar ratios Fluos-peptide/IAPP as indicated)) are shown for the following peptides: **(A)** IAPP; **(B)** 8A; **(C)** 4A; **(D)** A15,23,26; **(E)** A15,23; **(F)** A23,26; **(G)** A23; **(H)** A26; **(I)** A16. In the insets, the binding curves are shown; data are means ( $\pm$ SD) from three binding curves. Calculated app.  $K_{d}$ s are in Table 2.



**Supporting Figure S3.** Pull-down assay of Biotin-4A- and Biotin-IAPP-A $\beta$ 42 hetero-assemblies. Top: Anti-A $\beta$ 42 Western blot (WB) analysis of a mixture of A $\beta$ 42 (5  $\mu$ M) + Biotin-IAPP (2.5  $\mu$ M), a mixture of A $\beta$ 42 (5  $\mu$ M) + Biotin-4A (2.5  $\mu$ M), A $\beta$ 42 (5  $\mu$ M) alone, and Biotin-IAPP or Biotin-4A (2.5  $\mu$ M) alone as indicated following biotin pull-down and peptide dissociation from beads. Lane “A $\beta$ 42 control”, A $\beta$ 42 not incubated with beads. Bottom: Anti-Biotin WB of same incubations as in upper panel. Results shown are representative of 3 assays.

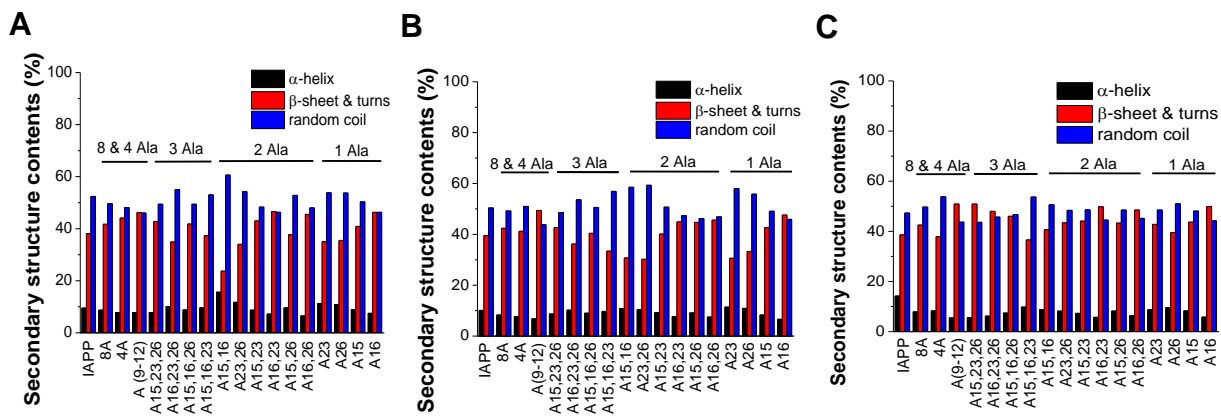


**Supporting Figure S4.** Effects of IAPP-GI and its Ala mutants on amyloidogenesis of A $\beta$ 40, A $\beta$ 42 and IAPP. **(A)** Effects on A $\beta$ 40 fibrillogenesis. Fibrillogenesis of A $\beta$ 40 (16.5  $\mu$ M) alone or with IAPP-GI, 4A-GI or A23-GI (1/1) were determined by the ThT binding assay. **(B)** Effects on A $\beta$ 42 fibrillogenesis. Fibrillogenesis of A $\beta$ 42 (16.5  $\mu$ M) alone or with IAPP-GI, 4A-GI or A15,23-GI (1/1) were determined by the ThT binding assay. **(C)** Effects on amyloidogenesis of IAPP. Fibrillogenesis of IAPP (12  $\mu$ M) alone or with IAPP-GI or 4A-GI (1/1) was followed by the ThT binding assay. All data shown in **(A-C)** are means ( $\pm$ SD) from 3 assays.



**Supporting Figure S5.** Solubilities of A15,23 and single Ala mutants at 50 and 20  $\mu\text{M}$ , respectively (aq. buffer, pH 7.4). Mutants were incubated for 7 days and solubilities were determined by a sedimentation assay (means ( $\pm\text{SD}$ ), 3 assays). Peptide amounts (% of total) in supernatants at 7 days of incubation are shown; a mutant is judged as soluble when  $\geq 80\%$  is found in supernatant (indicated by a dotted red line).





**Supporting Figure S6.** Calculated secondary structure contents of IAPP and mutants via deconvolutions of CD spectra at peptide concentrations of 5  $\mu\text{M}$  (**A**), 10  $\mu\text{M}$  (**B**) and 50  $\mu\text{M}$  (**C**).